IJMT. Vol. 22, Iss. 1, 2026. (66-79)

International Journal of Maritime Technology

Journal homepage: ijmt.ir

Comparison of Metaheuristic Algorithms for Weight Optimization of a Semi-Submersible VAWT Substructure with Hexagonal Pontoons

Zanyar Delgarm[1], Ahmad Reza Mostafa Gharabaghi[2*], Arefeh Emami[3]

[1] *M.Sc., Department of Civil Engineering, Sahand University of Technology, Tabriz, Iran; zanyardelgarm@gmail.com*
[2*] *Professor, Department of Civil Engineering, Sahand University of Technology, Tabriz, Iran; mgharabaghi@sut.ac.ir*
[3] *Assistant professor, Department of Civil Engineering, University of Hormozgan, Bandar Abass, Iran; emami@hormozgan.ac.ir*

ARTICLE INFO

Article History:
Received: 14 Jan 2026
Last modification: 17 Feb 2026
Accepted: 18 Feb 2026
Available online: 20 Feb 2026

Article type:
Article type

Keywords:
Metaheuristic optimization
Semi-submersible VAWT
Statistical evaluation algorithm
Hexagonal pontoons
Multi-criteria decision

ABSTRACT

In response to rising global energy demand and the urgent need to reduce greenhouse gas emissions, Offshore Wind Turbines (OWTs) have emerged as promising renewable energy solutions. Among deep-water support structures, semi-submersible platforms offer superior motion stability and design flexibility, but their high structural weight significantly affects construction and installation costs. This study compares five metaheuristic algorithms—Genetic Algorithm (GA), Ant Colony Optimization for Continuous Domains (ACO_R), Artificial Bee Colony (ABC), Firefly Algorithm (FA), and Particle Swarm Optimization (PSO)—for weight optimization of a four-column semi-submersible substructure supporting a Vertical Axis Wind Turbine (VAWT) with hexagonal pontoons. The algorithms were first validated with a reference platform optimized using the Generalized Reduced Gradient (GRG) method. They were then applied to minimize the VAWT substructure weight by optimizing pontoon and column geometry, spacing, and draft under hydrostatic stability, motion, airgap, and feasibility constraints. Each algorithm was executed five times, and Kolmogorov–Smirnov tests confirmed normality of optimized weight and Number of Function Evaluations (NFE). Analysis of Variance (ANOVA) indicated statistically significant differences among algorithms, and the Technique for Order of Preference by Similarity to Ideal Solution (TOPSIS) was used for multi-criteria decision-making, considering average weight, NFE, accuracy, variance, and stability. Results indicate that ACO_R achieved the highest rank, achieving ~37.6% (3690 tons) weight reduction. The findings demonstrate ACO_R's effectiveness as a decision-support tool for conceptual design of semi-submersible substructure of OWTs. However, it is expected that hydrodynamic loading, aero-structural coupling to be also considered for further detailed design.

ISSN: 2645-8136

DOI:

1. Introduction

With the increasing energy demand worldwide and the crucial obligations to decarbonization by 2050, offshore wind energy has appeared as a key solution in the transition to green energy resources [1]. The limitations of onshore wind resources and land-use competition have made it essential to focus on harvesting the vast potential of offshore wind. Statistics indicate that the installed capacity of offshore wind turbines will grow from 35.3 GW in 2020, to 2002 GW by 2050 [2]. This growth is particularly remarkable for semi-submersible turbines, whose capacity is projected to reach 1000 GW by 2050 [3]. Such growth highlights the increasing necessity for developing weight- and cost-optimized semi-submersible platforms.

The concept of floating platforms was first proposed by William Heronemus during 1972–1990 [4]. Unlike fixed platforms such as monopiles, which are constrained by water depth, floating structures can be installed at depths exceeding 60 meters while offering superior motion stability and greater design flexibility [5]. These advantages, combined with reduced operational costs in remote offshore locations, make floating platforms an ideal solution for offshore wind farm development. However, the inherent complexity of floating infrastructures in deep waters demands innovative design methodologies [6]. Park and Wang [7] investigated the hydrodynamic behavior of regular polygonal floating platforms, including triangular, square, hexagonal, and circular shapes, which revealed that with similar added mass, radiation damping, and dynamic response, polygonal geometries can lower mooring costs by improving wave dispersion. On the other hand, they facilitate the fabrication process [8].

Despite considerable progress in floating wind systems, semi-submersible substructures continue to pose challenges due to excessive weight, which raises construction, installation, and transportation costs though impairing dynamic performance [9]. While extra weight increases inertial forces, reduces power transmission efficiency, and restricts deployment in deeper waters [10], inappropriate weight reduction threatens stability, safety, and operational integrity [11]. This complex relationship between structural weight and performance necessitates sophisticated optimization approaches. Optimization methods are generally categorized into four groups: analytical, numerical, metaheuristic, and hybrid approaches. Analytical methods, based on differentiation and Karush-Kuhn-Tucker (KKT) conditions, are effective for convex problems with linear constraints but face limitations when dealing with nonlinear or multi-objective problems [12]. Numerical methods, on the other hand, require intensive computations as model complexity increases [13]. In contrast, metaheuristic methods have emerged as powerful tools for solving nonlinear and multi-objective problems with large solution spaces [14]. Notable examples include Particle Swarm Optimization (PSO) [15], Ant Colony Optimization (ACO) [16], Genetic Algorithm (GA) [17], Artificial Bee Colony (ABC) [18], and Firefly Algorithm (FA) [19]. Furthermore, hybrid methods combining the advantages of multiple approaches have been developed [20].

Extensive research has investigated the optimization of floating platforms and other types of substructures, including various approaches and applications. For example, Paulsen et al. [21] and Liu et al. [22] studied the design optimization of floating VAWTs. Karimi et al. [23] presented a multi-objective design optimization approach for FOWTs. Reyes-Casimiro et al. [24] developed an automatically optimized methodology for the structural design of a semi-submersible hull. Ivanov et al. [8] explored the shape optimization of columns and pontoons of FOWTs.

The selection of metaheuristic algorithms for structural optimization requires a comparative study. Therefore, the performance of different algorithms varies depending on the problem at hand.

While most previous studies on semi-submersible substructures have focused on Horizontal Axis Wind Turbines (HAWTs) and employed classical optimization methods with limitations in solving complex problems [25, 26], this study addresses these challenges through three key aspects, aiming to develop a lightweight and stable substructure for offshore wind energy applications: 1) it focuses on the design of VAWT substructures, taking into account their unique and geometrically challenging features in marine environments; 2) it conducts a systematic statistical comparison and ranking of five conventional metaheuristic algorithms (GA, ABC, FA, PSO, and ACO_R) for substructure weight optimization to identify the most suitable algorithm; 3) it introduces a four-column configuration with regular hexagonal pontoons, providing geometric symmetry that enables precise evaluation of algorithm performance on unconventional structures.

The article is structured as follows: following the introduction, Section 2 formulates the key parameters of the reference substructure, including geometric and hydrostatic properties, in a parametric manner, and introduces the metaheuristic algorithms considered in this study. Design constraints such as stability criteria, motion characteristics, ballast weight, and airgap were imposed. In Section 3, the developed algorithms and formulations are validated, and a detailed statistical comparison and ranking of the algorithms are presented. After selecting the most suitable algorithm, the output details of this algorithm are discussed. Finally, Section 4 provides the overall conclusions and suggestions for future research.

2. Research methodology

2.1. Selection and mathematical modeling of the substructure

2.1.1. Substructure selection

The optimization process in this study begins with the mathematical modeling of the floating substructure. The key design variables include the draft depth (with a constant distance from the still water level to the top of the column), dimensions of the columns and hexagonal pontoons, and distances between column centers. Parametric relationships have been developed to calculate the weight and problem constraints. In this regard, the case studied by Rajeswari and Nallayarasu [27] was considered. It was a four-column substructure with a Vertical Axis Wind Turbine (VAWT) installed on the central column which revealed better hydrodynamic responses compared to three-column substructures. The related specifications are shown in Fig. 1 and their values are presented in Table 1.

In this study, just the substructure of VAWT was considered, while the effect of turbine's weight and its center of gravity were accounted for hydrostatic stability analysis. As the primary objective of this study was to provide a simplified model for comparison of the performance of metaheuristic algorithms to serve as a decision tool for conceptual design, so the following simplification were adopted:

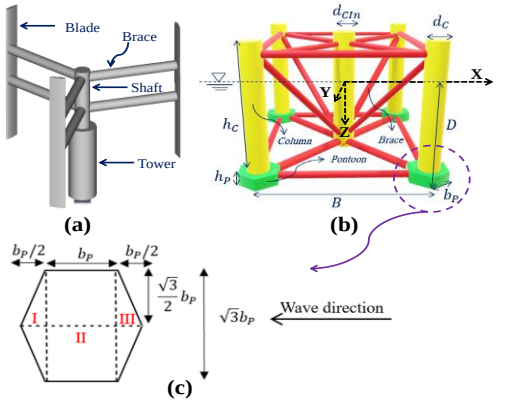

Figure 1. (a) Schematic view of VAWT; (b) Semi-submersible substructure with hexagonal pontoons; (c) Plan and segmentation of hexagonal pontoon into simpler shapes

Table 1. The primary details of VAWT & substructure [27]

Parameter	Symbol	Unit	Value
weight of VAWT	$W_{Turbine}$	kg	1539×10^3
COG of VAWT from keel	$G_{Turbine}$	m	30.80
Free board	F	m	12.75
Draft	D	m	24.75
Column diameter	d_C	m	11.25
Middle column diameter	d_{CIn}	m	6.75
Column height	h_C	m	30.00
Hexagonal pontoon edge length	b_P	m	12.37
Hexagonal pontoon height	h_P	m	7.50
Brace diameter	d_B	m	2.25
Displacement	Δ	kg	2.10×10^7
Center of gravity	COG	m	16.20
Metacentric height	GM	m	6.375
Moment of inertia about the x-axis	I_{xx}	$kg.m^2$	2.46×10^{10}
Damping	ξ	%	8.46
Natural period in heave motion	T_n^{Heave}	Sec	18.50
Added mass	A_{33}	kg	16650000

- As VAWTs have less tower sway and yaw mechanism compared to Horizontal Axis Wind Turbines (HAWTs) [28], so in this article, just heave motion was considered.
- Added mass of hexagonal pontoons was estimated using an empirical formulation.
- Bracing contribution was considered as a fixed proportion of the total displaced volume.
- Fatigue was not considered despite its negative effects on the lifetime of both types of HAWT and VAWT, but it is lower for VAWT because of its lower center of gravity [29].
- Stress control was not considered as the mass of VAWT is less than HAWT due, so HAWT is more affected by stress than the VAWT [29].

However, the following aspects are expected to be included in detailed design:

- VAWTs have the potential to produce the same amount of power as HAWTs with a lower average thrust and/or lower position of the Center of Pressure (CP), therefore imposing a lower inclining moment but substantially higher torque on the platform [30].
- Floating VAWTs experience increased motion in the frequency range close to the turbine [number of blades] × [rotational speed] frequency, which may overlap with the range of wave excitation forces for very large VAWTs with slower rotational speeds [30].

2.1.2. Displaced volume and displacement weight of substructure

The total displaced volume (∇_{Total}) was calculated as the sum of the underwater volumes of all substructure components as shown in Eq. (1), where $\nabla^P_{InWater}$, $\nabla^C_{InWater}$ and $\nabla^B_{InWater}$ represent the displaced volumes of the pontoon, column, and bracing members, respectively. These quantities were calculated according to Eq. (2) through Eq. (4). This formulation accounts for the full hydrostatic contribution of each submerged structural element while ensuring its geometric criteria.

The concept of the formulas and related parameters are inspired from the study of Gallala [31], who optimized the hull dimensions of a semi-submersible rig using the Generalized Reduced Gradient (GRG) method.

$$\nabla_{total} = \nabla^P_{InWater} + \nabla^C_{InWater} + \nabla^B_{InWater} \quad (1)$$

$$\nabla^P_{InWater} = 4\left(\frac{3\sqrt{3}}{2}b_P^2\right)h_P = 6\sqrt{3}h_P b_P^2 \quad (2)$$

$$\nabla^C_{InWater} = \pi\left[d_C^2(D-h_P) + \frac{1}{4}Dd_{CIn}^2\right] \quad (3)$$

$$\nabla^{B}_{InWater} = J_B\left(\nabla^{P}_{InWater} + \nabla^{C}_{InWater}\right) \quad (4)$$

The parameters are illustrated in Fig. 1b. Furthermore, for simplicity, the displaced volume of braces was considered as a fraction of the total displaced volume of the pontoons and columns (J_B), based on the initial structural configuration. Consequently, the bracing diameter was calculated using Eq. (5), where $L^{B}_{InWater}$ is the length of the brace submerged in the water.

$$d_B = \sqrt{\frac{4\nabla^{B}_{InWater}}{\pi L^{B}_{InWater}}} \quad (5)$$

Once the displaced volume was determined, the corresponding displaced weight (Δ) was calculated from Eq. (6), where ρ_w represents the water density.

$$\Delta = \rho_w \nabla_{total} \quad (6)$$

2.1.3. Heave's natural period

Heave and pitch motions are one the main challenges of VAWTs, so in this paper, the heave motion is considered. The heave's natural period was calculated from Eq. (7) where A_{33} is the added mass and A_w is the waterplane area. The damping is neglected in this equation. The added mass was calculated from Eq. (8) where C_m, the added mass coefficient which depends on the shape and dimensions of the pontoon. Given the hexagonal cross-section of the pontoon, it was divided into three sections I, II, and III according to Fig. 1c and the added mass was calculated separately for each section. In literature, the added mass coefficients for a two-dimensional rectangle with different length (a) to width (b) ratios are given [32]. So, by adapting them, an equation (Eq. 9) was derived for added mass coefficient. Then the results of each section were added together to ultimately yield Eq. (8).

When damping is considered, Eq. (10) is applied instead, where the damping ratio parameter ξ is taken as 8.46% [27].

The waterplane area of the substructure should be calculated as the summation of the cross-sectional areas of all water-piercing members, including columns and inclined diagonal bracing connected to the central column. In this study, due to the slight contribution of inclined diagonal braces and their complicated cross-sectional relation required to consider the change in the column height and draft depth, only the effect of columns was considered (Eq. 11). Later, it was noticed that such simplification has little effect on the results (refer to Fig. 2).

$$T_n^{Heave} = 2\pi\sqrt{\frac{\Delta + A_{33}}{\rho g A_w}} \quad (7)$$

$$A_{33} = C_m \rho V = 15.2341 \rho_w h_P^{1.148} b_P^{1.852} \quad (8)$$

$$C_m = 1.5488(a/b)^{-0.148} \quad (9)$$

$$T_D^{Heave} = \frac{T_n^{Heave}}{\sqrt{1-\xi^2}} \quad (10)$$

$$A_w = \pi\left(d_C^2 + \frac{d_{CIn}^2}{4}\right) \quad (11)$$

2.1.4. Ballast weight

During the calculations, in order to keep a constant freeboard, water ballast was used to adjust the draft depth. It was assumed that the water ballast was filled only inside the pontoons. Accordingly, the ballast weight was calculated from Eq. (12), where t is the member thickness, $h_{Ballast}$ is the ballast water height and b_P is the width of the pontoons. By substituting b_P from Table 1 and the density of water from Table 2, the final relation was obtained.

$$\begin{aligned} w_{Ballast} &= 6\sqrt{3}(b_P - 2t)^2 h_{Ballast} \times \rho_w \\ &= h_{Ballast}[1590198.27 \\ &- (514211.24 \times t) \\ &+ (4569.22 \times t^2)] \end{aligned} \quad (12)$$

This equation expresses the ballast weight as a quadratic function of both parameters and is applicable when $h_{Ballast}$ is known. Alternatively, the ballast weight can also be determined using Eq. (13), based on the turbine weight ($W_{Turbine}$), the displaced weight (Δ) and the platform weight ($W_{Platform}$).

$$w_{Ballast} = \Delta - w_{Platform} - w_{Turbine} \quad (13)$$

In this context, $W_{Platform}$ was defined as the sum of the weights of all platform components (columns, pontoons, and braces) as shown in Eq. (14), which was calculated under the assumption that all structural members are made from steel (ρ_{St}). The weight of individual components can be calculated using Eq. (15) to Eq. (17).

$$w_{Platform} = w_P + w_C + w_B \quad (14)$$

$$\begin{aligned} w_C = \Big[&\left(4\pi h_C(d_C t - t^2)\right) \\ &+ \left(\pi(h_C + h_P)(d_{CIn} t - t^2)\right) \\ &+ \left(\pi t(d_C^2 + 0.25 d_{CIn}^2)\right)\Big]\rho_{St} \end{aligned} \quad (15)$$

$$\begin{aligned} w_P = \Big[&\left(24\sqrt{3} h_P(b_P t - t^2)\right) \\ &+ \left(12\sqrt{3} b_P^2 t\right)\Big]\rho_{St} \end{aligned} \quad (16)$$

$$w_B = \left[4\pi L^{B}_{total}(d_B t - t^2)\right]\rho_{St} \quad (17)$$

Thus, the ballast weight can be expressed as Eq. (18).

$$\begin{aligned} w_{Ballast} = &72945732.5t^2 - 248059764.5t \\ &- 19461000 \end{aligned} \quad (18)$$

By equating Eq. (12) and (18), Eq. (19) can be derived.

$$(72945732.5 - 4569.22h_{Ballast})t^2 - (248059764.5 - 514211.24h_{Ballast})t + (19461000 - 1590198.27h_{Ballast}) = 0 \quad (19)$$

In this study, it was assumed that 80% of pontoon's capacity is filled, resulting in a member thickness of 4 cm.

2.1.5. Substructure's center of gravity (COG)

The substructure's COG can be estimated from Eq. (20), where, m_P , m_C and m_B are the moments generated by different components of the substructure.

$$d^{keel-COG} = \frac{m_P + m_C + m_B}{w_P + w_C + w_B} \quad (20)$$

The moment arms and related moments induced by the pontoons, columns, and bracing members are given in Eq. (21) through Eq. (26).

$$d_P^{keel-COG} = \frac{1}{2}h_P \quad (21)$$

$$m_P = w_P d_P^{keel-COG} \quad (22)$$

$$d_C^{keel-COG} = \frac{\sum w_i d_{C(i)}^{keel-COG}}{\sum w_i} \quad (23)$$

$$m_C = w_C d_C^{keel-COG} \quad (24)$$

$$d_B^{keel-COG} = \frac{\sum w_i d_B^{keel-COG}}{\sum w_i} \quad (25)$$

$$m_B = w_B d_B^{keel-COG} \quad (26)$$

2.1.6. Second moment of area

In operational conditions, the second moment of area for the waterplane surface is calculated based on the columns. The considered structure is symmetric about the horizontal and vertical axes in plan view; therefore, the longitudinal and transverse second moments of area are the same and is calculated by Eq. (27).

$$I = \frac{\pi}{64}(4d_C^4 + 16d_C^2B^2 + d_{CIn}^4) \quad (27)$$

2.1.7. Vertical distance between COB and MC

Due to the symmetry about both horizontal and vertical axes, the vertical distance between the center of buoyancy (COB) and metacenter (MC) is identical for both longitudinal and transverse directions and can be obtained from Eq. (28).

$$d^{COB-MC} = \frac{I}{\nabla} \quad (28)$$

2.1.8. Vertical distance from the COB to the keel

The vertical distance from the COB to the keel equals the ratio of the moment generated by the displaced weight to the displaced weight itself. Alternatively, the displaced volume can be used instead of the displaced weight, according to Eq. (29).

$$d^{keel-COB} = \frac{(d^{P,COB} \times \nabla^P) + (d^{C,COB} \times \nabla^C) + (d^{B,COB} \times \nabla^B)}{\nabla^P + \nabla^C + \nabla^B} \quad (29)$$

The COB of individual structural components was calculated from Eq. (30) through Eq. (32).

$$d^{P,COB} = \frac{1}{2}h_P \quad (30)$$

$$d^{C,COB} = \frac{\sum \nabla_i^C d_i^{C,COB}}{\sum \nabla_i^C} \quad (31)$$

$$d^{B,COB} = \frac{\sum \nabla_i^B d_i^{B,COB}}{\sum \nabla_i^B} \quad (32)$$

2.1.9. Vertical distance between the COG and MC

For stability, any floating structure must have a positive GM (distance between the COG and the MC). Since the distance between the COB and MC is identical in both longitudinal and transverse directions, the longitudinal and transverse GM values are estimated from Eq. (33).

$$GM = d^{keel-COB} + d^{COB-MC} - d^{keel-COG} \quad (33)$$

2.2. Constraints

2.2.1. Stability constraints

To ensure adequate stability, any floating vessel must satisfy the positive GM condition, at the same time, engineers avoid excessively high GM Values, since they cause undesirable short rolling periods appeared by increased reaction forces and accelerations (Eq. 34).

$$GM_{min} \leq GM \leq GM_{max} \quad (34)$$

2.2.2. Constraint for motion characteristics

Safe operation in harsh marine environments requires constraints on motion characteristics of the floating structure. The most critical motion is heave oscillations [33], whose magnitude depends on the heave natural period. Eq. (35) ensures that the heave natural period remains above a specified minimum threshold.

$$T^{Heave} \geq T_{Min}^{Heve} \quad (35)$$

2.2.3. Ballast weight constraint

The ballast water quantity is a critical parameter for achieving the target freeboard (vertical distance from water surface to column top) and suitable draft depth. The ballast mass must be positive, while the ballast water volume in the pontoons is limited by the pontoon capacity as expressed in Eq. (36), where parameter Z is considered to be 80% of the pontoon's capacity.

$$w_{Ballast} \leq \left(\rho_w 6\sqrt{3}h_P b_P^2\right)Z \qquad 0 \leq Z \leq 1 \quad (36)$$

2.2.4. Stability constraints

Freeboard (F) is a critical parameter for semi-submersible to prevent wave-in-deck loads. This

constraint imposed by Eq. (37) to ensure adequate freeboard during operation.

$$h_C + h_P - D = F \quad (37)$$

2.2.5. Geometric constraints

In addition, several geometric constraints were imposed in this study to preserve the initial structural configuration and ensure the feasibility of the optimization process. Also, structural dimensions were bounded by upper and lower limits based on existing similar structures. The constraints of construction and fabrication was also considered.

Table 2 summarizes the parameter values applied during the optimization process. $G_{Turbibe}$ denotes the vertical distance from the top of the column to the COG of the turbine.

Table 2. The primary details of VAWT & substructure [27]

Parameter	Value	Parameter	Value
ρ_w	1000 [kg/m^3]	J_B	0.06 [-]
ρ_{St}	7850 [kg/m^3]	$G_{Turbine}$	30.8 [m]
G	9.806 [kg/m^3]	Z	0.8 [-]
b_P^{Max}	20 [m]	U	0.9 [-]
b_P^{Min}	8 [m]	F	12.75 [m]
h_P^{Max}	15 [m]	GM_{Max}	4 [m]
h_P^{Min}	5 [m]	GM_{Min}	1.5 [m]
d_C^{Max}	20 [m]	B_{Max}	100 [m]
d_C^{Min}	8 [m]	B_{Min}	35 [m]
h_C^{Max}	50 [m]	R_{Max}	3 [-]
h_C^{Min}	20 [m]	R_{Min}	1 [-]
T_{Min}^{Heave}	18.5 [sec]	D_{Max}	40 [m]
t	0.04 [m]	D_{Min}	15 [m]

2.3. Metaheuristic algorithms

All metaheuristic algorithms were implemented with a maximum iteration stopping criterion and penalty function (csv=1×10¹²) for constraint handling. The GA was executed using MATLAB's optimization toolbox for its computational efficiency and to avoid the convergence challenges often encountered in manual implementations. The other four algorithms, ACO_R, PSO, FA, and ABC were custom-coded.

The ACO algorithm, which was introduced in the 1990s [34-36], simulates the intelligent foraging behavior of ants in identifying the shortest path to food sources [18]. In 2008, Socha and Dorigo [37] presented a fundamental progress by introducing the continuous ACO_R framework, in which pheromones are represented by a normal distribution function and an archive of high-quality solutions guides the search process. This study adopts that approach, with parameters set as: maximum iterations = 9000, archive size = 20, number of samples = 100, selection pressure = 0.35, and Deviation-Distance Ratio = 1.

The GA, inspired by natural evolution principles, employs selection, crossover, and mutation mechanisms to explore the design space [15]. In this study, the optimization parameters were set as follows: initial population size = 500 chromosomes, maximum generations = 2000, crossover rate = 80%, and mutation rate = 20%. An arithmetic crossover operator was used, generating offspring as weighted linear combinations of parent solutions.

The PSO algorithm simulates the collective behavior of birds, utilizing particle positions and velocities to explore the search space [16]. Key parameters were set to: maximum iterations = 5000, swarm size = 100, and cognitive/social coefficients - both set to 2.05.

The FA simulates the phototropic behavior of insects [20], utilizing light intensity (objective function) and light absorption ($\beta = 2$) parameters. Other parameters were: maximum iterations = 5000, population size = 10 fireflies, randomization coefficient = 0.2, and damping ratio for randomization coefficient = 0.99.

The ABC algorithm, inspired by the intelligent foraging behavior of honeybees [19], was implemented with a population of 50 scout bees and a maximum of 5000 iterations. The algorithm employed three bee groups: 25 worker bees for selected sites, 10 onlooker bees for elite sites, and scout bees exploring the design space using the uniform bee dance operator, gradually reducing the search radius with coefficient = 0.99.

The key hyperparameters used in the metaheuristic algorithms of this study are summarized in Table 3.

Table 3. Parameters of the studied metaheuristic algorithms

Algorithm	Population / Archive	Max Iterations	Key Parameters
GA	500	2000	Crossover = 0.8, Mutation = 0.2
PSO	100	5000	$c_1 = c_2 = 2.05$
FA	10	5000	$\beta = 2$, $\alpha = 0.2$, Damping = 0.99
ABC	50	5000	Limit coefficient = 0.99
ACO_R	20	9000	Samples = 100, q = 0.35

2.4. Comparison of algorithms

The final evaluation of the metaheuristic algorithms was conducted based on five key indicators: 1) average weight of results, 2) average Number of Function Evaluations (NFE), 3) relative accuracy of solutions, 4) stability, and 5) reliability. Additional secondary criteria, including decision variable outcomes and computational time, were also assessed. Relative accuracy was defined as the ratio of the minimum result obtained among the five algorithms to the solutions of each algorithm. Stability was expressed as the inverse of the coefficient of variation (1/CV) of weight results, while reliability was represented by the variance of weight results. Initial comparisons of algorithms were made using these criteria, followed by an investigation of whether the differences were due to their stochastic nature or inherent algorithmic characteristics. The Kolmogorov-Smirnov (K-S) test confirmed the normal distribution of each algorithm's outputs across five

independent runs, thereby permitting the application of parametric statistical tests, namely ANOVA and Tukey. ANOVA was employed to determine the significance of overall differences, while Tukey's test was used for pairwise comparisons of algorithms; a significance level of 5% was considered for both of them. Finally, the TOPSIS method, which is described in section 3.5, was applied to perform the final ranking of the algorithms [38, 39].

Although a larger number of independent runs would further enhance statistical robustness, five runs per algorithm were selected as a trade-off between computational cost and statistical validity. The implications of limited sample size are reflected in the reported variance and discussed as a limitation.

3. Results and Discussion

3.1. Validation

Before executing the coded algorithms for optimizing the semi-submersible wind turbine substructure, validation process was conducted not only for the developed formulations but also for the generated coded algorithms. Fig. 2 demonstrates the validation results obtained by applying the reference VAWT and related substructure parameters [27] to the developed formulations (presented in section 2). This includes verification of the damped heave natural period, vertical distance between the COG and MC, added mass, displaced weight, and stiffness. There is good agreement between the calculated results and their physical quantities. In this case, the initial structural weight was estimated about 9,802 tons.

Afterwards, for validation of the generated coded algorithms, the drilling rig model which was optimized by Gallala [31] using the GRG method under transit, operational, and survival conditions (shown in Fig. 3) utilized as the benchmark case study. For brevity, only the outputs of ACO_R are shown in Fig. 4 and the results obtained from all of the studied algorithms are presented in Table 4. The GRG-based benchmark results were reproduced in MATLAB under identical geometric constraints reported by Gallala [31]. Default solver configurations were retained to maintain methodological consistency, and no additional parameter tuning was introduced in the reproduction process. The optimal weight obtained using ACO_R is 7,954 tons, approximately 1.73% lower than the 8,083 tons reported using the GRG method. This is an acceptable difference between the reproduced weight and the reported GRG method. This confirms the reliability of the developed formulations and coded algorithms, however, due to the stochastic nature of metaheuristic algorithms, exact repetition of reference study's results was not expected.

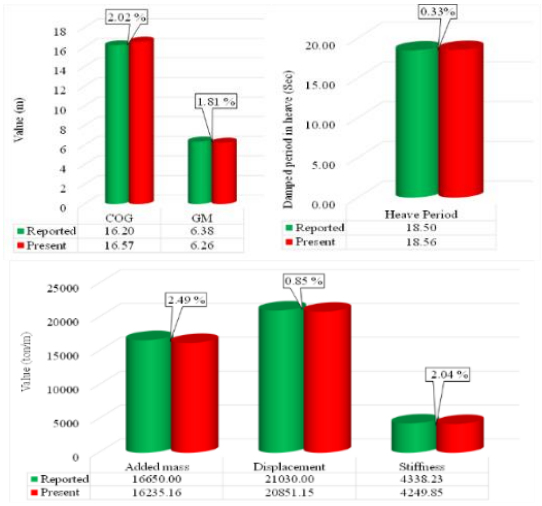

Figure 2. Validation of the developed mathematical formulations

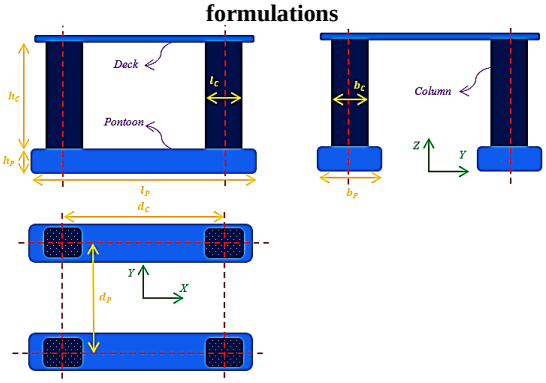

Figure 3. Schematic configuration of drilling rig proposed by Gallala [31] with rectangular pontoons and columns

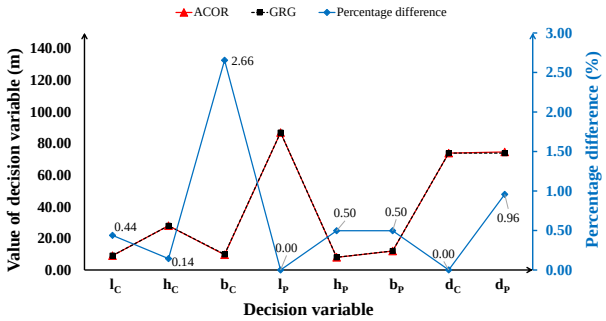

Figure 4. Validation of the ACO_R through comparison of the results with the GRG method [31]

Table 4. Results for decision variables of the drilling rig obtained from the generated algorithms

Algorithm	ACO_R	PSO	BA	FA	GA	GRG
l_C (m)	9.07	9.11	9.28	8.86	10.23	9.11
h_C (m)	28.00	28.00	28.20	28.00	28.00	27.96
b_C (m)	9.66	9.62	9.26	9.89	8.81	9.92
l_P (m)	87.00	87.00	91.16	87.00	87.00	87.00
h_P (m)	8.00	8.00	7.80	8.00	8.00	8.04
b_P (m)	12.00	12.00	11.70	12.00	12.06	12.06
d_C (m)	74.00	74.00	74.77	74.00	72.93	74.00
d_P (m)	74.68	75.08	76.36	75.56	73.61	73.97
Weight (t)	7954	7954	7901	7955	8068	8093
Difference with GRG	1.71 %	1.72 %	2.38 %	1.71 %	0.31 %	-

3.2. Evaluation of algorithms

3.2.1. Comparing the performance of metaheuristic algorithms

After validation of the generated coded algorithms, they were implemented for optimization of the decision variables of the substructure of studied VAWT [27]. The results are shown in Fig. 5 which supports almost similar quantities. The difference is mainly observed for the column height, resultant draft and their distance to each other. In the next step, these five metaheuristic algorithms were evaluated through five independent runs aimed at minimizing the weight of the VAWT substructure. As illustrated in Fig. 6, although the decision variable results in Fig. 5 appear almost similar, but meaningful differences in substructure weight is observed. This highlights that the importance of design parameters is different in marine structure's weight optimization. Furthermore, it seems that the dispersion of the results is different for the studied metaheuristic algorithms. The optimized weight results from each independent run, their standard deviation (STD) and their mean value for each algorithm are summarized in Table 5. It confirms that the ACO_R algorithm achieved the best performance with an average weight of 6,112 tons, while ABC produced the worst results of mean weight of 6,694 tons. It also reveals the ACO_R's smaller standard deviation (STD) compared to other algorithms which indicates its significant higher reliability.

Although, from some viewpoint, computational time may be more important criterion, but the number of function evaluations (NFE) required to neutralize the penalty function, as a measure for convergence speed, can be more suitable which is shown in Fig. 7. Performance differences arise from the distinct search mechanism employed by each algorithm within the design space.

In addition to NFE, the average computational time over five independent runs was recorded. Although execution time depends on hardware specifications and implementation environment, the recorded averages (GA: 59 s, ABC: 5 s, FA: 10 s, PSO: 13 s, ACO_R: 26 s) provide complementary insight into practical computational cost. Nevertheless, NFE was retained as the primary convergence indicator due to its hardware-independent nature.

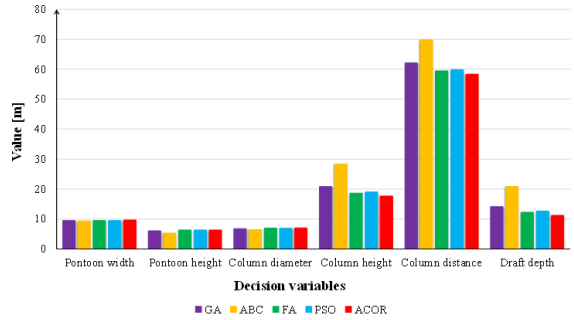

Figure 5. Optimized decision variables for substructure of VAWT obtained by the studied algorithms

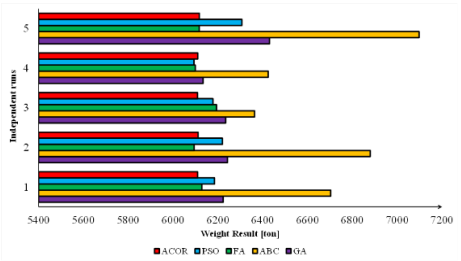

Figure 6. Discrepancy in the weight of substructure obtained from five independent runs of each algorithm

The evaluation of algorithm efficiency based on the NFE reveals that the FA presented the fastest convergence with NFE of 16,200. In contrast, the GA exhibited the slowest performance with a NFE of 607,400, highlighting the inherent benefit of intelligent search mechanisms like those in FA compared to GA. As noticed in the overdrawn section of Fig. 7, although GA's final results fall within an acceptable range, its high NFE prior to full convergence is notable. This is further supported by GA's gradual, downward-sloping convergence curve during the final stages.

Table 5. Optimized weight results, their STD and mean value from five independent runs of each algorithm

Run No.	(ton)				
	GA	ABC	FA	PSO	ACO_R
1	6223.81	6703.56	6128.42	6184.84	6109.82
2	6242.78	6880.32	6094.02	6220.41	6111.83
3	6235.09	6363.95	6194.06	6178.20	6109.22
4	6133.93	6424.18	6099.027	6093.06	6110.17
5	6430.39	7097.70	6116.82	6307.62	6117.20
STD	108	308	40	78	3
Mean weight	6253	6694	6126	6197	6112

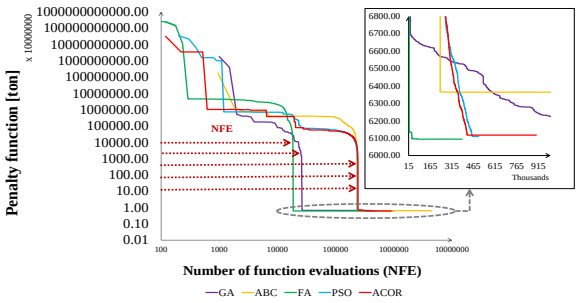

Figure 7. Optimization and convergence trend of algorithms, displaying the criterion for NFE

3.2.2. Accuracy of optimal solutions and stability of algorithms

The relative accuracy of the algorithms, assessed by the average solution ratio shown in Fig. 8a, indicates that the ABC algorithm has the lowest precision, likely due to its short search process, and Fig. 8b presents the stability coefficient, defined as the ratio of average optimal weight to standard deviation, which shows that ACO_R is the most stable algorithm, with a stability

coefficient of 1,879. Hence the key question arises whether these differences in results and NFE metrics are simply due to the stochastic nature of the algorithm, or does the choice of the algorithms fundamentally affect the optimization results? To address this, data normality was first verified by the K-S test shown in Fig. 9. All algorithms exhibited K-S statistics below the critical value of 0.56327 at the 5% significance level [40], validating the use of parametric ANOVA and Tukey tests.

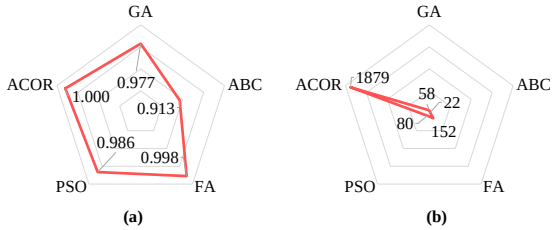

Figure 8. (a) Accuracy and (b) Stability of optimization algorithms in 5 iterations.

3.3. ANOVA test results

Analysis of variance (ANOVA) test for final weight of platform and NFE criteria are presented in Tables 6 and 7 respectively, which shows F-statistic of 12.63 and 9.85 for the final platform's weight and NFE criteria, individually, both exceeding the critical value of 2.866. This indicates that the null hypothesis (H_0), assuming equal means for these two criteria is refused. Significant level of $P = 5\%$ was adopted in this study. The calculated p-values were 2.75×10^{-5} for the optimized platform weight and 1.43×10^{-4} for NFE, both substantially below the 5% significance threshold. Given that the Kolmogorov–Smirnov test confirmed normality of the samples, the application of parametric ANOVA is statistically justified despite the limited number of independent runs.

In other words, ANOVA demonstrated that the probability of differences in the scattered output results is below 5%, confirming statistically significant differences among the algorithms. Thus, the variations discussed in the previous sections are not due to algorithmic randomness (H_1), but rather arise from the intrinsic mechanisms of the algorithms. Specifically, ANOVA indicated that at least one algorithm in this study differs from the others, and its inclusion or exclusion in substructure optimization could fundamentally alter the results. Consequently, the ANOVA outcomes necessitate pairwise comparisons of algorithms, which are addressed in the following section.

Table 6. ANOVA test results for optimized weight data of studied algorithms in five different runs

Source of Variation	Between Groups	Within Groups	Total
SS	1154171.981	457037.307	1611209.289
df	4	20	24
MSE	288542.995	22851.865	
F	12.627		
P-value	2.753E-05		
F_{Crit}	2.866		

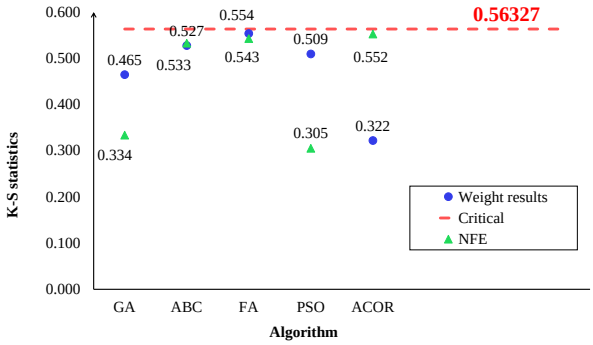

Figure 9. Comparing the K-S statistics with its critical value in the Kolmogorov-Smirnov test for weight and NFE results

3.4. Pairwise comparison of algorithms (Tukey)

The pairwise comparison of the studied algorithms are presented in Table 8 which is the absolute difference between two results obtained from each algorithm. If this difference exceeds the value $HSD = q \times \sqrt{MSE/n}$, it is considered statistically significant and highlighted in red. In this expression, MSE denotes the mean square error obtained from the ANOVA test, n is the number of samples in each group (n=5), and q is the studentized range distribution based on error, which, for n, number of groups (k=5), and a 5% significance level, HSD is calculated as 4.232 from the corresponding values of q obtained from its related tables [42]. Although software such as SPSS or R can be used for this analysis, Excel is applied in this study. The Tukey test shows that, for the substructure weight criterion, the ABC algorithm is significantly different from the others, while no statistically significant difference is observed among FA, PSO, and ACO_R algorithms. Regarding the NFE criterion, results indicate that only GA is significantly different from the other algorithms, with no notable difference among the other four algorithms. These findings highlight that although some algorithms such as GA and ABC clearly demonstrate lower performance, the others including FA, PSO, and ACO_R are statistically at the same level and can be considered suitable alternatives.

Table 7. ANOVA test results for NFE data of studied algorithms in five different runs

Source of Variation	Between Groups	Within Groups	Total
SS	1.054E+12	5.348E+11	1.589E+12
df	4	20	24
MSE	2.634E+11	2.674E+10	
F	9.851		
P-value	1.428E-04		
F_{Crit}	2.866		

3.5. Ranking algorithms using the TOPSIS method

To comprehensively evaluate the performance of the studied algorithms, the Technique for Order of Preference by Similarity to Ideal Solution (TOPSIS) method, a Multi-Criteria Decision-Making (MCDM) technique was applied. The values of the criteria and their assigned weights (C.W.) are presented in Table 9. Criteria weights were assigned based on engineering judgment, prioritizing structural weight reduction as the primary objective. Considering that the mean optimized weights obtained from the five algorithms are relatively close in magnitude, moderate variations in the weight assigned to the primary objective are not expected to alter the overall ranking outcome.

The final weight of each criterion was obtained by combining their relative weights [43]. The authors assigned values from 1 to 9 to each criterion based on the "Combined relative weighting" section of Table 9 and the importance of each criterion, as reported in the "Relative weight" row of the same table. These values were then divided pairwise in Table 10 and normalized in Table 11. Finally, the final weight of each criterion, presented under the designation C.W., was calculated by averaging the values of each row in Table 11.

This approach evaluates the algorithms based on five key criteria: average optimal weight, NFE, dispersion of weight results, accuracy, and model stability. TOPSIS facilitates comparison and selection of the best option by calculating the distance of each algorithm from the positive ideal solution and the negative ideal solution. For all criteria, except relative accuracy and stability, the positive ideal corresponds to the minimum value obtained by the algorithms, while the negative ideal corresponds to the maximum; this condition is reversed for accuracy and stability. Based on the TOPSIS ranking results shown in Table 12, ACO_R, with a similarity index of 0.881, was identified as the best algorithm. This superiority was mainly attributed to achieving the lowest platform weight (7970 tons), combined with the highest accuracy, stability, and reliability, although the number of NFE in this algorithm is higher compared to PSO and FA. FA and PSO ranked second and third, respectively, whereas GA and ABC, with weaker performance, are positioned in the lower ranks. These findings clearly reveal ACO_R as the preferred option for this engineering problem, despite higher computational demands, due to its substantial advantages across other criteria. The following sections present the algorithm results in detail.

3.6. ACO_R results

3.6.1. Accuracy of optimal solutions and stability of algorithms

Multiple runs demonstrated the model's capability to satisfy all constraints with 5,000 iterations and a population size of 20. The model was further tested by increasing the iterations up to 10,000. As shown in Fig. 10 the optimized weight in all cases was lower than the initial weight, with convergence achieved after approximately 8,000 iterations. As mentioned earlier, in this study, the maximum number of iterations for the ACO_R algorithm was considered to be 9000. It should be noted that the other algorithms were assigned maximum iterations in a similar manner.

All optimized configurations satisfied the predefined hydrostatic stability, ballast, freeboard, and geometric feasibility constraints imposed in the optimization model. Although detailed structural strength and fatigue verification were beyond the scope of the present work, the resulting geometric dimensions fall within ranges reported for comparable semi-submersible platforms in the literature.

3.6.2. VAWT substructure results from the ACO_R

Due to the stochastic nature of the model, as reported in Table 13, multiple executions yield different but valid results, all satisfying the constraints. On average, a 37.6% weight reduction (approximately 3,686 tons) was observed. The standard deviation, around 0.05% (3 tons), demonstrates the proposed model's reliability across different runs. This consistency, despite the stochastic nature, confirms the algorithm's capability to identify stable optimal solutions.

Table 8. Tukey tests for optimized weight and average NFE results in five independent runs

Algorithm	GA	ABC	FA	PSO	ACO_R
Average weight results					
GA	-	440.741	126.733	56.375	141.553
ABC	440.741	-	567.747	497.116	582.294
FA	126.733	567.747	-	70.358	14.821
PSO	56.375	497.116	70.358	-	85.179
ACO_R	141.553	582.294	14.821	85.179	-
Average NFE results					
GA	-	328890	591199	522740	342860
ABC	328890	-	262309	193850	13970
FA	591199	262309	-	68459	248339
PSO	522740	193850	68459	-	179880
ACO_R	342860	13970	248339	179880	-

Table 9. Decision criteria used in the TOPSIS method and their relative weights

	Avg. weight [ton]	Avg. NFE	Variance	Accuracy	Stability
GA	6253.2	607400	11730.61	0.977	57.735
ABC	6694.0	278510	94878.00	0.913	21.732
FA	6126.5	16200	1617.40	0.998	152.321
PSO	6196.8	84660	6022.45	0.986	79.851
ACO_R	6111.7	264540	10.58	1.000	1879.142
Relative weight	9	3	5	7	6
C.W.	0.328	0.098	0.149	0.229	0.196
Combined relative weighting					
Option A	9 8 7 6 5 4 3 2 1	2 3 4 5 6 7 8 9			**Option B**

Table 10. Pairwise division weight of criteria

	Avg. weight [ton]	Avg. NFE	Variance	Accuracy	Stability
Avg. weight [ton]	1.000	3.000	3.000	1.286	1.500
Avg. NFE	0.333	1.000	0.600	0.429	0.500
Variance	0.556	1.000	1.000	0.714	0.833
Accuracy	0.778	2.333	1.400	1.000	1.167
Stability	0.667	2.000	1.200	0.857	1.000
Sum	3.333	9.333	7.200	4.286	5.000

Table 11. Normalized pairwise weights and final weight of criteria

	Avg. weight [ton]	Avg. NFE	Variance	Accuracy	Stability	C. W.
Avg. weight [ton]	0.300	0.321	0.417	0.300	0.300	0.328
Avg. NFE	0.100	0.107	0.083	0.100	0.100	0.098
Variance	0.167	0.107	0.139	0.167	0.167	0.149
Accuracy	0.233	0.250	0.194	0.233	0.233	0.229
Stability	0.200	0.214	0.167	0.200	0.200	0.196
Sum	1.000	1.000	1.000	1.000	1.000	1.000

Table 12. Ranking results of metaheuristic algorithms based on the TOPSIS method

	Similarity index				Rank
Alg.	D_i^+	D_i^-	$D_i^+ + D_i^-$	P_i	
GA	0.206	0.130	0.337	0.387	4
ABC	0.246	0.045	0.291	0.153	5
FA	0.179	0.167	0.347	0.482	2
PSO	0.187	0.156	0.344	0.455	3
ACO_R	0.034	0.248	0.282	0.881	1

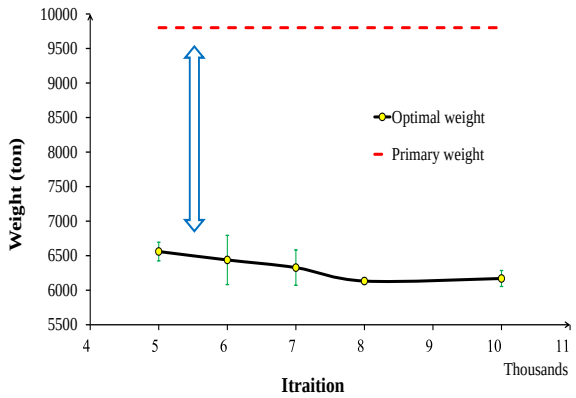

Figure 10. Comparison of primary [27] and optimized weights with standard deviation of optimization results in five runs

4. Conclusion

This study developed a parametric framework to evaluate five metaheuristic algorithms (GA, ACO_R, ABC, FA, PSO) for optimizing a semi-submersible VAWT substructure with hexagonal pontoons. The optimization process adhered to constraints of hydrostatic stability, motion performance, geometric feasibility, and airgap. Each algorithm was executed five times, and the K-S test confirmed that the results followed a normal distribution. The findings are summarized as follows:

1) Overall, ANOVA, at a 5% significance level, indicated that the choice of algorithm had a statistically significant effect on optimization results, and the differences observed were not due to randomness but were attributable to the mechanisms and inherent characteristics of the algorithms.

2) Specifically, Tukey's test revealed that the ABC algorithm, in terms of structural weight, and the GA algorithm, in terms of NFE, significantly differed from the others, with these differences reflecting their inferior performance relative to the rest.

3) The final ranking using the TOPSIS method, based on criteria of average weight, average NFE, relative accuracy, stability, and reliability, identified the ACO_R algorithm as the best method, achieving a 37.6% reduction in structural weight (from the initial 9802

tons to 6112 tons), despite requiring higher computational effort compared to PSO and FA.
4) The FA, PSO, GA, and ABC algorithms ranked next, respectively.
5) Furthermore, it was shown that, comparatively, ACO_R exhibited superior relative accuracy (100%), stability (1/CV = 1879.142), and reliability (Variance = 10.58) compared to the others.
The main limitations of this study include simplified hydrodynamic modeling, neglect of aero-structural coupling, and the absence of detailed structural strength assessment. Future research should incorporate fully coupled time-domain simulations, multi-objective optimization frameworks, and extended statistical sampling for detailed design.

5. Author Contribution

Z. Delgarm: Writing – original draft, Visualization, Validation, Methodology, Investigation, Data curation.
A.R. Mostafa Gharabaghi: Writing – review & editing, Supervision, Methodology, Conceptualization.
A. Emami: Writing – review & editing, Supervision.

6. Data Availability Statement

Data will be made available on request.

Table 13. Results of decision variables from the ACO_R algorithm

Try	Pontoon width	Pontoon height	Column diameter	Column height	distance of column	Depth draft	Substructure weight	Avg. weight	Reduced weight	Standard deviation
	[m]						[ton]	[ton]	[%]	[ton]
1	9.44	6.83	6.83	20.20	61.13	13.53	6109.817			
2	9.63	6.32	7.01	17.49	58.15	11.06	6111.827			
3	9.61	6.31	7.00	17.67	58.36	11.23	6109.217	6112	37.64	3
4	9.62	6.30	7.00	17.67	58.37	11.22	6110.174			
5	9.66	6.35	7.004	17.14	57.75	10.74	6117.202			

7. References

1- Karimirad, M. (2014). Offshore energy structures: for wind power, wave energy and hybrid marine platforms. Springer.
2- Bilgili, M., & Alphan, H. (2022). Global growth in offshore wind turbine technology. Clean Technologies and Environmental Policy, 24(7), 2215-2227. http://dx.doi.org/10.21203/rs.3.rs-1202466/v1
3- Amani, S., Prabhakaran, A., & Bhattacharya, S. (2023, June 12-14). Seismic Performance Assessment of Floating Offshore Wind Turbines supported by Tension Leg Platforms. 9th ECCOMAS Thematic Conference on Computational Methods in Structural Dynamics and Earthquake Engineering, Greece. http://dx.doi.org/10.7712/120123.10398.20788
4- Reddy, K. T., Chaitanya, J. S. N., Chandramouli, K., & Kumar, M. C. N. (2021). A Study on Floating Wind Turbine for Offshore Power Generation. Journal for Modern Trends in Science & Technology, 7 (0707078), 236-240. http://dx.doi.org/10.46501/IJMTST0707039
5- Ahn, H., Ha, Y. J., & Kim, K. H. (2023). Load evaluation for tower design of large floating offshore wind turbine system according to wave conditions. Energies, 16(4), 1862. https://doi.org/10.3390/en16041862
6- Ojo, A. (2024). Geometric shape parameterization and optimization of floating offshore wind turbine substructure within an MDAO framework. https://doi.org/10.48730/6db0-5693
7- Park, J. C., & Wang, C. M. (2021). Hydrodynamic behaviour of floating polygonal platforms under wave action. Journal of Marine Science and Engineering, 9(9), 923. https://doi.org/10.3390/jmse9090923
8- Ivanov, G., Hsu, I. J., & Ma, K. T. (2023). Design considerations on Semi-Submersible columns, bracings and pontoons for floating wind. Journal of Marine Science and Engineering, 11(9), 1663. https://doi.org/10.3390/jmse11091663
9- Wang, J., Ren, Y., Shi, W., Collu, M., Venugopal, V., & Li, X. (2025). Multi-objective optimization design for a 15 MW semisubmersible floating offshore wind turbine using evolutionary algorithm. Applied Energy, 377, 124533. https://doi.org/10.1016/j.apenergy.2024.124533
10- Drabo, S., Lai, S., Liu, H., & Feng, X. (2024). 10 MW FOWT Semi-Submersible Multi-Objective Optimization: A Comparative Study of PSO, SA, and ACO. Energies, 17(23), 5914. https://doi.org/10.3390/en17235914
11- Sahu, S.K., Kumar, V., Dutta, S.C., Sarkar, R., Bhattacharya, S., & Debnath, P. (2024). Structural safety of offshore wind turbines: Present state of knowledge and future challenges. Ocean Engineering, 309, 118383. http://dx.doi.org/10.1016/j.oceaneng.2024.118383
12- Arora, R. K. (2015). Optimization: algorithms and applications. CRC press. https://doi.org/10.1201/b18469
13- Nocedal, J., & Wright, S.J. (1999). Numerical optimization. New York, NY: Springer New York.
14- Benaissa, B., Kobayashi, M., Al Ali, M., Khatir, T., & Elmeliani, M.E.A.E. (2024). Metaheuristic optimization algorithms: An overview. HCMCOU

Journal of Science–Advances in Computational Structures, 33-61. http://dx.doi.org/10.46223/HCMCOUJS.acs.en.14.1.47.2024

15- Kennedy, J., & Eberhart, R. (1995). Particle swarm optimization. In Proceedings of ICNN'95-International Conference on Neural Networks (Vol. 4, pp. 1942-1948). IEEE. http://dx.doi.org/10.1109/ICNN.1995.488968

16- Dorigo, M., & Blum, C. (2005). Ant colony optimization theory: A survey. Theoretical Computer Science, 344(2-3), 243-278. https://doi.org/10.1016/j.tcs.2005.05.020

17- Mathew, T. V. (2012). Genetic algorithm. Report submitted at IIT Bombay, 53, 18-19. http://dx.doi.org/10.22541/au.159164762.28487263

18- Bansal, J. C., Sharma, H., & Jadon, S. S. (2013). Artificial bee colony algorithm: a survey. International Journal of Advanced Intelligence Paradigms, 5(1-2), 123-159. http://dx.doi.org/10.1504/IJAIP.2013.054681

19- Fister, I., Fister Jr, I., Yang, X.S., & Brest, J. (2013). A comprehensive review of firefly algorithms. Swarm and Evolutionary Computation, 13, 34-46. https://doi.org/10.1016/j.swevo.2013.06.001

20- Zukhri, Z., & Paputungan, I.V. (2013). A hybrid optimization algorithm based on genetic algorithm and ant colony optimization. International Journal of Artificial Intelligence & Applications, 4(5), 63-75. http://dx.doi.org/10.5121/ijaia.2013.4505

21- Paulsen, U.S., Madsen, H.A., Hattel, J.H., Baran, I., & Nielsen, P.H. (2013). Design optimization of a 5 MW floating offshore vertical-axis wind turbine. Energy Procedia, 35, 22-32. http://dx.doi.org/10.1016/j.egypro.2013.07.155

22- Liu, Q., Bashir, M., Huang, H., Miao, W., Xu, Z., Yue, M., & Li, C. (2025). Nature-inspired innovative platform designs for optimized performance of Floating Vertical Axis Wind Turbines. Applied Energy, 380, 125120. https://doi.org/10.1016/j.apenergy.2024.125120

23- Karimi, M., Hall, M., Buckham, B., & Crawford, C. (2017). A multi-objective design optimization approach for floating offshore wind turbine support structures. Journal of Ocean Engineering and Marine Energy, 3, 69-87. https://link.springer.com/article/10.1007/s40722-016-0072-4

24- Reyes-Casimiro, M., Félix-González, I., & Perea, T. (2023). Design optimization for production semi-submersible pontoons based on genetic algorithms and finite element analysis. Ocean Engineering, 268, 113291. http://dx.doi.org/10.1016/j.oceaneng.2022.113291

25- Otter, A., Murphy, J., Pakrashi, V., Robertson, A., & Desmond, C. (2022). A review of modelling techniques for floating offshore wind turbines. Wind Energy, 25(5), 831-857. https://doi.org/10.1002/we.2701

26- Patryniak, K., Collu, M., & Coraddu, A. (2022). Multidisciplinary design analysis and optimisation frameworks for floating offshore wind turbines: State of the art. Ocean Engineering, 251, 111002. https://doi.org/10.1016/j.oceaneng.2022.111002

27- Rajeswari, K.S., & Nallayarasu. (2021). Hydrodynamic response of three-and four-column semi-submersibles supporting a wind turbine in regular and random waves. Ships and Offshore Structures, 16(10), 1050-1060. http://dx.doi.org/10.1080/17445302.2020.1806681

28- Gupta, S.K., Pandey, A.P., Sawla, A., Baredar, P. (2016). A Brief Review on Design and Performance Study of Vertical Axis Wind Turbine Blades. International Research Journal of Engineering and Technology (IRJET), 3(7), 465-471

29- Al-Rawajfeh, M.A. & Gomaa, M.R. (2023). Comparison between horizontal and vertical axis wind turbine. International Journal of Applied Power Engineering (IJAPE), 12(1), 13-23. DOI: 10.11591/ijape.v12.i1.pp13-23

30- Borg, M. & Collu, M. (2014). A comparison between the dynamics of horizontal and vertical axis offshore floating wind turbines. Phil. Trans. R. Soc. A 373: 20140076. http://dx.doi.org/10.1098/rsta.2014.0076

31- Gallala, J.R. (2013). Hull Dimensions of a Semi-Submersible Rig: A Parametric Optimization Approach. Master's thesis, Institutt for marin teknikk.

32- Patel, M.H. (2013). Dynamics of offshore structures. Butterworth-Heinemann.

33- DNV, G. (2004). DNV-OS-J101–Design of offshore wind turbine structures. DNV GL.

34- Dorigo, M. (1992). Optimization, learning and natural algorithms. Ph.D. Thesis, Politecnico di Milano.

35- Dorigo, M., Maniezzo, V., & Colorni, A. (1996). Ant system: optimization by a colony of cooperating agents. IEEE Transactions on Systems, Man, and Cybernetics, Part B (Cybernetics), 26(1), 29-41. http://dx.doi.org/10.1109/3477.484436

36- Dorigo, M., Di Caro, G., & Gambardella, L.M. (1999). Ant algorithms for discrete optimization. Artificial Life, 5(2), 137-172. http://dx.doi.org/10.1162/106454699568728

37- Socha, K., & Dorigo, M. (2008). Ant colony optimization for continuous domains. European Journal of Operational Research, 185(3), 1155-1173. https://doi.org/10.1016/j.ejor.2006.06.042

38- Rehman, S., Khan, S.A., & Alhems, L.M. (2020). Application of TOPSIS approach to multi-criteria selection of wind turbines for on-shore sites. Applied Sciences, 10(21), 7595. https://doi.org/10.3390/app10217595

39- Krohling, R.A., & Pacheco, A.G. (2015). A-TOPSIS–an approach based on TOPSIS for ranking evolutionary algorithms. Procedia Computer Science, 55, 308-317. http://dx.doi.org/10.1016/j.procs.2015.07.054

40- Facchinetti, S. (2009). A procedure to find exact critical values of Kolmogorov-Smirnov test. Statistica Applicata–Italian Journal of Applied Statistics, 21(3-4), 337-359.

41- Johnson, N.L., Kotz, S., & Balakrishnan, N. (1995). Continuous univariate distributions, volume 2 (Vol. 2). John wiley & sons.

42- Abdi, H., & Williams, L.J. (2010). Newman-Keuls test and Tukey test. Encyclopedia of research design, 2, 897-902.

43- Ezzat, A.E., & Hamoud, H.S. (2016). Analytic hierarchy process as module for productivity evaluation and decision-making of the operation theater. Avicenna journal of medicine, 6(01), 3-7. https://doi.org/10.4103/2231-0770.173579